B.Tech Project (Stage II) Report:

Probabilistic Edge Tuning of Boolean Networks to Influence Cell Fate

Shabnam Sahay
190050111

Supervisor: Prof. Ganesh Viswanathan
Co-supervisor: Prof. Ashutosh Gupta

IIT Bombay

April 2023

1 Introduction

Several biological processes are controlled by networks of interacting genes, proteins, transcription factors, signalling molecules, and other biological entities. Modelling and performing simulations on these networks can aid in obtaining an understanding of the conditions that drive their dynamics to certain states - for example, the differences in conditions that drive a TNF-activated cell to apoptosis versus necroptosis (non-apoptotic cell death).

Boolean dynamic networks are a commonly used model for such biological networks. When modelling them in boolean form, each entity is represented by a single node which can either have an ON (1) or OFF (0) value. The value of each entity at a given time is determined by the value of its 'neighbouring' entities which interact with it, either activating or inhibiting it. Such relationships can be encoded into a boolean logic function that takes as input the values of these other entities and outputs the value of the entity in consideration.

Extensive work has been done to construct such boolean models reflecting biological phenomena and perform simulations to determine attractors, steady-state probabilities, and other metrics which can help uncover the behaviour and dynamics of real biological systems. In particular, the roles of different nodes in driving cells to specific fates is one such area of interest.

The input of TNFα to a biological network can lead a cell to any of three cell fates or phenotypes - survival, non-apoptotic cell death (hereafter referred to as nonACD), and apoptosis. It is known that knocking out a node (for example, an entity such as RIP1) from the network can change the probability of a cell reaching each of these fates (i.e. absorption probability), and consequently the distribution of steady-state probabilities in a cell population. However, due to biological cross-talk, the complete deletion of a node is not physically feasible.

This partial inhibition of interactions of these nodes with other nodes can be simulated in a boolean network through probabilistic edge tuning [1]. Here, the inhibition of particular network edges is carried out via edge tuning, in order to:

(i) observe whether resulting changes in absorption probabilities for various cell fates correspond to data known from experiments,

(ii) identify initial network states where specific perturbations increase apoptosis probability without significantly affecting survival probability, and

(iii) determine which node(s) in the network play a key role in making a particular state very sensitive to edge-tuning, with respect to the amount that its apoptosis absorption probability shifts relative to its survival absorption probability.

2 Boolean dynamic networks

2.1 Notation

Consider a network B with n nodes $a_1, a_2, \ldots, a_n$. Each node a_i has a corresponding boolean value which varies as a function of time as $v_i(t)$. $\forall t \in \mathbb{N}$ and $\forall i \in \{1, 2, \ldots, n\}$, $v_i(t)$ can take either the value 0 or 1. The state of the network B at time t is uniquely represented by the binary string $V(t) = v_1(t)v_2(t)\cdots v_n(t)$.

$v_i(t)$ is determined by a boolean function f_i that takes as input the values of a set M_i of m_i nodes at time t'. While the time t' is dependent on the update scheme used (explained in more detail below), f_i itself has a specified functional form that is independent of the update scheme.

$$v_i = f_i(M_i) = f_i(v_k \forall a_k \in M_i) \text{ where } M_i = \{a_{i1}, a_{i2}, \ldots, a_{im_i}\} \tag{1}$$

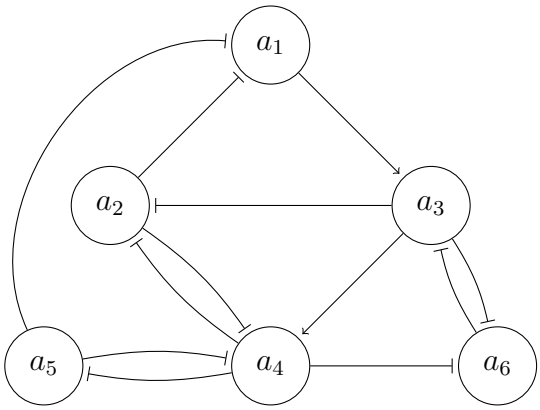

Figure 1: A six-node network from [2], corresponding to TGFβ signalling in cancer cells. Nodes $a_1, a_2, a_3, a_4, a_5, a_6$ denote TGFβ, miRNA200, Snail1, Zeb1, Ovol2, and miRNA34a respectively. A $\rightarrow$ connection represents activation and $\dashv$ connection represents inhibition.

f_i	M_i	$f_i(M_i)$
f_1	$\{a_2, a_5\}$	$\neg v_2 \vee \neg v_5$
f_2	$\{a_3, a_4\}$	$\neg v_3 \vee \neg v_4$
f_3	$\{a_1, a_6\}$	$v_1 \wedge \neg v_6$
f_4	$\{a_2, a_3, a_5\}$	$v_3 \wedge \neg v_2 \wedge \neg v_5$
f_5	$\{a_4\}$	$\neg v_4$
f_6	$\{a_3, a_4\}$	$\neg v_3 \vee \neg v_4$

Table 1: f_i, M_i and $f_i(M_i)$ for the 6-node network shown in 1.

2.2 Update schemes

$V(t)$ depends on the value of each of its constituent nodes. Depending on whether these values are updated simultaneously (all nodes together) or step-by-step (one node after another), there are three update schemes commonly used in boolean dynamic networks:

1. Synchronous update

   All $v_i(t)$ values are computed in a simultaneous update, by considering the values of all the nodes in their respective M_i sets at time $t-1$.

   $$v_i(t) = f_i(v_{i1}(t-1), v_{i2}(t-1), \ldots, v_{im_i}(t-1)) \forall i \in \{1, \ldots, n\} \tag{2}$$

2. Ordered asynchronous update

   Let the period of time between $t-1$ and t be broken down into n smaller equally-spaced intervals, separated by the time markers $t_1, t_2, \ldots, t_n$ where $t_n = t$. Let $t_0 = t-1$.

   v_1 is updated at time t_1 using the values of all nodes as they originally are at $t_0 = t-1$. Thus at t_1, v_1 has an updated value, while the values of all other nodes simply carry over to remain the same as they were at t_0.

Next, v_2 is updated at time t_2 using the values of all nodes as they are at t_1. Thus, if $a_1 \in M_2$, v_2 is updated using the previously updated value v_1.

Similarly, at each time t_i, v_i is updated using the values of all nodes as they are at t_{i-1}, and uses the already updated values of nodes $a_1, \ldots, a_{i-1}$ to do so.

Thus the value of the nodes is updated step-by-step here in a well-defined order.

3. Random-order asynchronous (ROA) update

   The difference between this update scheme and the ordered asynchronous update scheme is only in the order in which the nodes are updated step-by-step. Whereas the latter has a well-defined update order, here a random ordering of the nodes is chosen in which to perform the updates.

   With n nodes in the network, there are hence $n!$ different possible update orders which can be chosen for every update from $V(t-1)$ to $V(t)$.

2.3 Steady-state probabilities

A state transition graph (STG) captures the one-step transition probabilities between all possible pairs of states of the network. A network with n nodes will have 2^n possible states, hence an adjacency matrix representation of an STG will be a $2^n \times 2^n$ matrix S. S_{ij} then denotes the probability of a one-step transition from the ith state to the jth state occurring.

Clearly, these probabilities will be dependent on the update scheme used. A synchronous update scheme defines a single possible end-state for a one-step transition from a given start-state of the network, leading to the construction of a binary-valued S.

However, an ROA update scheme, which considers $n!$ possible different orders in which to update the values of the nodes, usually leads to more than one possible end-state for a one-step transition from a given start-state. In this case, S_{ij} is calculated by finding the number of permutations (update orders) that lead to state j from state i, and dividing this by $n!$.

Every Boolean network has particular states called fixed points or attractors dependent on the update scheme being utilized [3]. Updating the network when it is in one of these states will result in it remaining in the same state, i.e. all possible one-step transitions from that state lead to itself. Hence the network is said to attain steady state when it reaches any attractor.

The steady-state probability (SSP) of an attractor is the probability that, if the network is initialized to a random state, it will attain steady state in that particular attractor. Determining the SSPs of various attractors of a network, as well as its STG, can be useful in understanding and making further inferences about its behaviour.

3 Understanding cell fate on a singe-cell level

3.1 Constructing STGs using BM-ProSPR

An ROA update scheme is likely to be more biologically relevant than a synchronous one, since all participating entities in the network are unlikely to update their value at exactly the same instant in time. Moreover, the order in which they will update in a real system is not deterministic, making ROA update more pertinent than an ordered asynchronous update.

Given a network B with n nodes, the state space of the network is 2^n. To construct a complete $2^n \times 2^n$ STG for this network with an ROA update scheme, the total number of permutations to be considered for each one-step transition is $n!$. Since $n!$ grows much faster than 2^n (Figure 2), the bottleneck of constructing the STG with ROA updates at large n becomes the consideration of all possible permutations for each one-step transition.

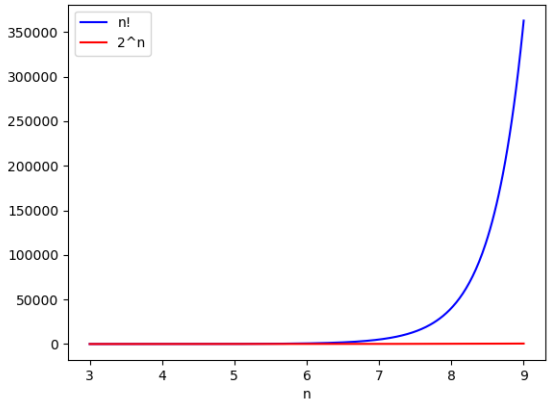

Figure 2: The number of permutations required to consider all possible orders in an ROA update scheme ($n!$) grows much faster than the state space of a network with n nodes (2^n).

A possible approach to tackle this is to consider only a subset of these $n!$ permutations, working under the assumption that increasing the number of permutations used beyond a point will not significantly change the calculated transition probabilities of the network.

The BM-ProSPR algorithm [4] implements this approach. It computes a minimum number of permutations Q, with which when we perform ROA on the given network from all of its starting states, generates an STG that is a reasonable estimate of the true STG of the network.

BM-ProSPR is thus used here to construct the STG of considered boolean networks under a random order asynchronous (ROA) update scheme, which subsequently allows calculation of the steady-state probabilities (SSPs) of a cell population and absorption probabilities of individual initial states.

3.2 Absorption probabilities

In order to understand the probabilities of achieving a certain cell fate (i.e. steady state) on a single-cell level, absorption probabilities are useful. In contrast to steady-state probabilities, which correspond to an average over all the possible initial states that a cell population can take, absorption probabilities correspond to a single initial network state, and how likely it is to reach each of the three possible steady states.

Given an n node network, it has 2^n initial states, with a $2^n \times 2^n$ STG M. Taking a square diagonal matrix A with all diagonal entries $= 1/n$ and remaining entries $= 0$, an integer value t can be found such that $AM^t \sim AM^{t+1}$. Then the absorption probability of the ith state to the jth state can be found in the (i, j)th entry of AM^t. This value will only be non-zero if the jth state is a fixed point, corresponding to a particular cell fate in the current context.

4 Influencing and quantifying shift in cell fate

4.1 Network edge inhibition

It has been demonstrated in experiments that knocking out a node from a network can change the distribution of its steady state probabilities, and thus the distribution of absorption probabilities of individual states too. However, due to biological cross-talk, the complete deletion of a node is not practical - some indirect influence is retained.

To reflect this kind of partial inhibition of network edges in a boolean model, a probabilistic edge tuning approach proposed by Deritei et al. [1] is followed. This method encodes 'noise' in boolean network edges by introducing probabilistic edge-weight (PEW) operators, which enable incomplete inhibition of particular edges in the network being modelled.

Taking the network in 1 as an example, suppose the edge desired to be tuned is the edge from node a_3 to a_4. The boolean rule that governs v_4, the value taken by a_4, is given by $v_4 = v_3 \wedge \neg v_2 \wedge \neg v_5$ in the unchanged network. Let the edge tuning parameter be denoted by $\theta \in [0, 1]$. This represents the degree to which the $a_3 \to a_4$ edge is inhibited. The inhibition is encoded into the boolean rule governing v_4 as follows:

Algorithm 4.1: To be carried out each time the node a_4 is to be updated.

Input: θ
Sample p from $U(0, 1)$
if $p < \theta$ **then**
  Update a_4 using the rule $v_4 = \neg v_2 \wedge \neg v_5$,
  else Update a_4 using the rule $v_4 = v_3 \wedge \neg v_2 \wedge \neg v_5$
end

If $\theta = 0$, there is zero edge inhibition - the value of a_3 always influences the value of a_4 during an update step. If $\theta = 1$, there is complete edge inhibition - the value of a_3 never (directly) influences the value of a_4 during an update step.

4.2 Quantifying shift in cell fate probabilities

Apoptosis is a kind of 'silent death' - when a cell dies via apoptosis, the surrounding cells are not aware and do not get affected. However, when cells die via NonACD, they cause inflammation in their surroundings, which is especially detrimental in a tumor environment. It is hence desirable to identify modifications in boolean network models of cancer cells that shift the steady-state probabilities (and absorption probabilities) such that increased apoptosis and decreased nonACD is observed, with minimally-affected survival response.

Quantifying this shift in absorption probabilities for each initial network state allows us to identify those states that are most sensitive, and thus those network nodes that are critical in effecting the shift.

For a given initial state s in the wild-type network WT, let its survival absorption probability and apoptosis absorption probability be $ABP_{Survival}(WT, s)$ and $ABP_{Apoptosis}(WT, s)$ respectively. For the state s in an edge-tuned network WT, let its survival absorption probability and apoptosis absorption probability be $ABP_{Survival}(ETN, s)$ and $ABP_{Apoptosis}(ETN, s)$ respectively.

$$\Delta ABP_{Survival}(s) = |ABP_{Survival}(ETN, s) - ABP_{Survival}(WT, s)| \tag{3}$$

$$\Delta ABP_{Apoptosis}(s) = |ABP_{Apoptosis}(ETN, s) - ABP_{Apoptosis}(WT, s)| \tag{4}$$

The objective of identifying initial network states where specific perturbations increase apoptosis probability without significantly affecting survival probability can then be achieved by finding network states s among the selected initial states where $\Delta ABP_{ratio}(s)$ is maximized:

$$\Delta ABP_{ratio}(s) = \frac{\Delta ABP_{Apoptosis}(s)}{\Delta ABP_{Survival}(s)} \tag{5}$$

5 Eleven-node network

5.1 Network definition

In [5], Calzone et al. describe a boolean network utilized to model cell-fate decisions. The nodes of this network are shown in Figure 3, with the corresponding boolean rules in Table 2.

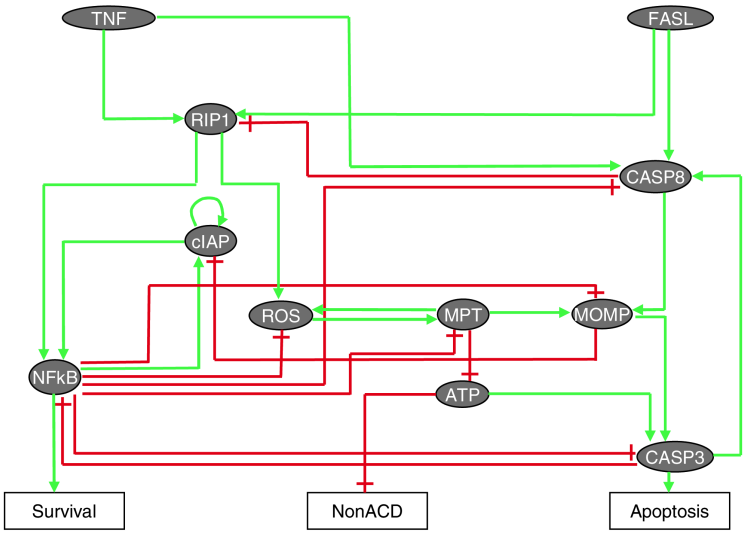

Figure 3: The eleven-node network described in [5] which models interactions influencing the three cell fates - survival, non-apoptotic cell death and apoptosis.

Node	Boolean rule
TNF	Input node (always set to ON)
FAS	Input node (always set to OFF)
$RIP1$	$\neg C8 \wedge (TNF \vee FAS)$
$NFkB$	$(cIAP \wedge RIP1) \wedge \neg C3$
$C8$	$(TNF \vee FAS \vee C3) \wedge \not{NFkB}$
$cIAP$	$(NFkB \vee cIAP) \wedge \neg MOMP$
ATP	$\neg MPT$
$C3$	$ATP \wedge MOMP \wedge \not{NFkB}$
ROS	$\neg NFkB \wedge (RIP1 \vee MPT)$
$MOMP$	$MPT \vee (C8 \wedge \neg NFkB)$
MPT	$ROS \wedge \not{NFkB}$

Table 2: Boolean rules of the 11-node network shown in Figure 3. TNF and FAS are input nodes that are always set to 1 and 0 respectively in this work.

5.2 RIP1 → ROS edge tuning

Considering the WT network in Figure 3, BM-ProSPR is run with $TNF = 1$ and $FAS = 0$ to generate the STG and thus calculate the absorption probability to the three steady states Survival (S), NonACD (N), and Apoptosis (A) for each of the 512 initial network states. The obtained distribution of absorption probabilities is shown in Figure 4.

Working with the assumption that edge inhibition cannot be complete, we tune the $RIP1 \rightarrow ROS$ edge with $\theta = 0.8$. The resulting distribution of absorption probabilities after running BM-ProSPR on this network is shown in Figure 5.

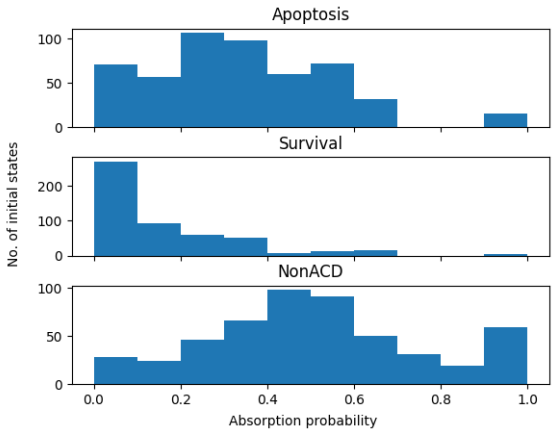

Figure 4: Distribution of absorption probabilities for all 512 initial states of the wild-type network in Figure 3 with $TNF = 1$ and $FAS = 0$. STG for the network was generated as an average of 20 re-initializations of BM-ProSPR.

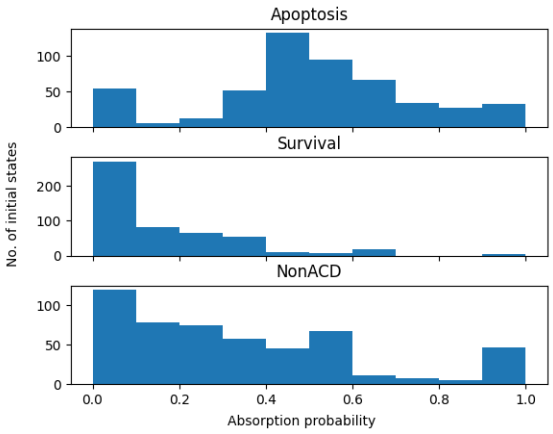

Figure 5: Distribution of absorption probabilities for 512 initial states of the network with $RIP1 \rightarrow ROS$ edge tuned with $\theta = 0.8$. STG for the tuned network was generated as an average of 20 re-initializations of BM-ProSPR.

Comparing the two figures, an overall increase in $ABP_{Apoptosis}$ can be seen. This is compensated by a decrease in ABP_{NonACD}, with no significant change visible in $ABP_{Survival}$.

This is repeated for all values of $\theta \in \{0.0, 0.1, 0.2, 0.3, \ldots, 0.9, 1.0\}$. As θ increases, a monotonic right-ward shift of the $ABP_{Apoptosis}$ distribution is seen, along with a monotonic left-ward shift of the ABP_{NonACD} distribution. This increase of apoptosis probability with respect to survival probability on inhibition of the direct $RIP1 \rightarrow ROS$ interaction is consistent with results seen in existing literature.

5.3 TNF → C8 edge tuning

The same process is carried out with a perturbed network where the tuned edge is $TNF \rightarrow CASP8$ with $\theta = 0.8$. The absorption probability distributions for all 512 states in the WT and perturbed network can be seen in Figures 6 and 7 respectively.

Here, there is a clear overall decrease of $ABP_{Apoptosis}$ compensated by an increase in ABP_{NonACD}, with negligible change in the distribution of $ABP_{Survival}$ once again.

This is repeated for all values of $\theta \in \{0.0, 0.1, 0.2, 0.3, \ldots, 0.9, 1.0\}$. As θ increases, a monotonic left-ward shift of the $ABP_{Apoptosis}$ distribution is seen, along with a monotonic right-ward shift of the ABP_{NonACD} distribution, and $ABP_{Survival}$ remaining relatively unaffected. These results are also consistent with those seen in existing literature.

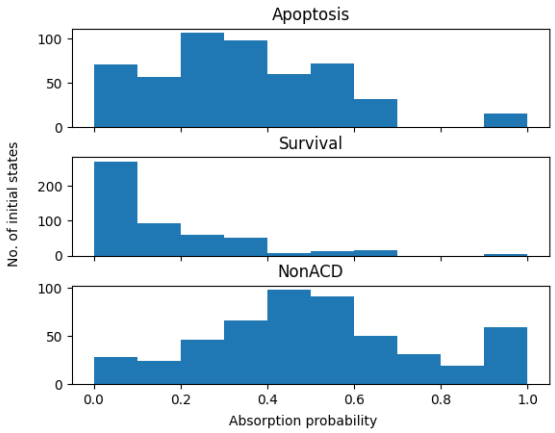

Figure 6: Distribution of absorption probabilities for all 512 initial states of the wild-type network in Figure 3 with $TNF = 1$ and $FAS = 0$. STG for the network was generated as an average of 20 re-initializations of BM-ProSPR.

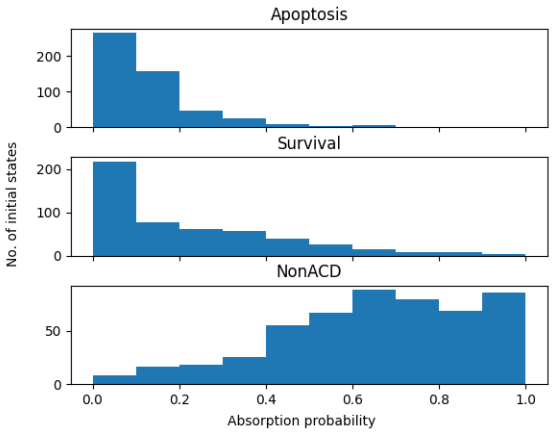

Figure 7: Distribution of absorption probabilities for 512 initial states of the network with $TNF \rightarrow C8$ edge tuned with $\theta = 0.8$. STG for the tuned network was generated as an average of 20 re-initializations of BM-ProSPR.

5.4 Simultaneous tuning of RIP1 → ROS and TNF → C8 edges

Inhibition of the $RIP1 \rightarrow ROS$ edge increases $ABP_{Apoptosis}$ with respect to $ABP_{Survival}$, and inhibition of the $TNF \rightarrow C8$ edge decreases it. Next, a network with both edges simultaneously perturbed is considered, taking $\theta = 0.8$ and 0.2 for these edges respectively, since the objective is to maximize the increase of $ABP_{Apoptosis}$ with respect to $ABP_{Survival}$.

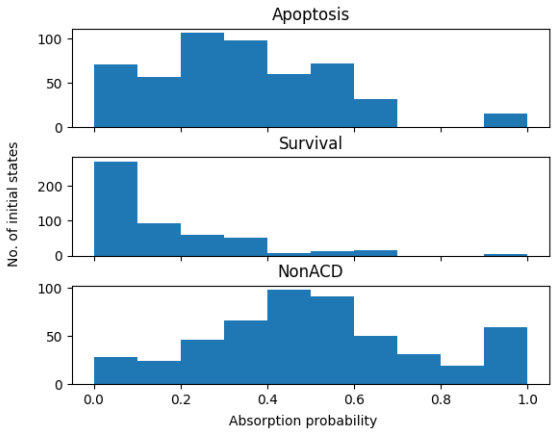

Figure 8: Distribution of absorption probabilities for all 512 initial states of the wild-type network in Figure 3 with $TNF = 1$ and $FAS = 0$. STG for the network was generated as an average of 20 re-initializations of BM-ProSPR.

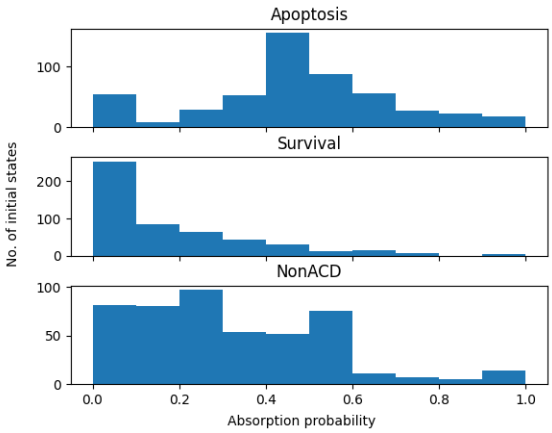

Figure 9: Distribution of absorption probabilities for 512 initial states with $RIP1 \rightarrow ROS$ edge tuned with $\theta = 0.8$ and $TNF \rightarrow C8$ edge tuned with $\theta = 0.2$. STG was generated as an average of 20 BM-ProSPR re-initializations.

5.5 Selecting initial network states for analysis of shift in cell fate

To further analyze those initial states in particular that are biologically relevant, i.e. their absorption probabilities reflect those seen in experiments, we select those states s in the WT network such that:

$$ABP_{Survival}(WT, s) \geq ABP_{Apoptosis}(WT, s) \geq ABP_{NonACD}(WT, s) \quad (6)$$

This condition is fulfilled by the following 22 out of the 512 initial network states. These states are denoted as $S_0, S_1, S_2, \ldots, S_{20}, S_{21}$ in the following analysis.

State index	State	State index	State
S0	10010100000	S11	10110110100
S1	10010100100	S12	10111100000
S2	10010101000	S13	10111100001
S3	10010110000	S14	10111100100
S4	10010110100	S15	10111100101
S5	10010111000	S16	10111100110
S6	10100100000	S17	10111110000
S7	10100110000	S18	10111110001
S8	10110100000	S19	10111110100
S9	10110100100	S20	10111110101
S10	10110110000	S21	10111110110

Table 3: The 22 initial states of the network in Figure 3 that fulfil Equation 6.

The shift in the distribution of absorption probabilities for only these 22 states on carrying out edge tuning of $RIP1 \rightarrow ROS$ with $\theta = 0.8$ is checked. Relative to the WT network (Figure 10), we again see an overall increase in $ABP_{Apoptosis}$ compensated by a decrease in ABP_{NonACD} in the edge-tuned network (Figure 11), with less significant changes in $ABP_{Survival}$.

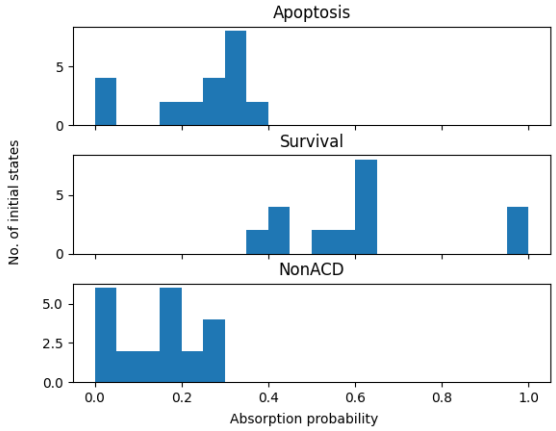

Figure 10: Distribution of absorption probabilities for 22 selected initial states of the wild-type network with $TNF = 1$ and $FAS = 0$. STG for the network was generated as an average of 20 re-initializations of BM-ProSPR.

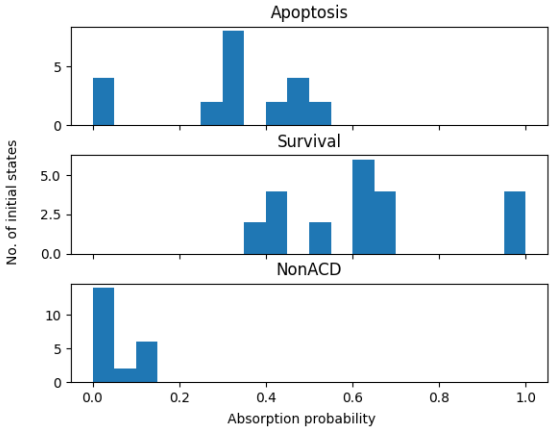

Figure 11: Distribution of absorption probabilities for 22 selected initial states of the network with $RIP1 \rightarrow ROS$ edge tuned with $\theta = 0.8$. STG for the tuned network was generated as an average of 20 BM-ProSPR re-initializations.

Repeating the same for the case with edge tuning of $TNF \rightarrow C8$ with $\theta = 0.8$, a similar shift to that observed when all 512 initial states were considered is seen.This can be seen on comparing Figure 13 with Figure 12.

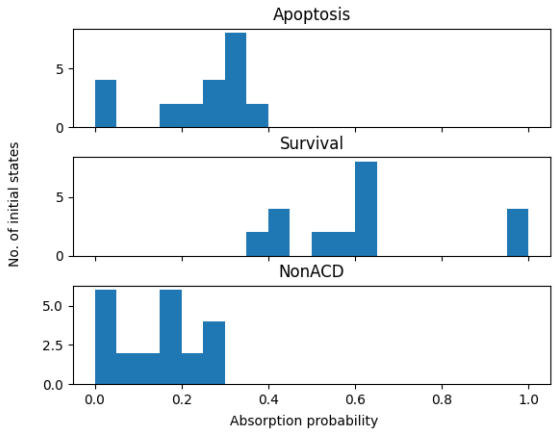

Figure 12: Distribution of absorption probabilities for 22 selected initial states of the wild-type network with $TNF = 1$ and $FAS = 0$. STG for the network was generated as an average of 20 re-initializations of BM-ProSPR.

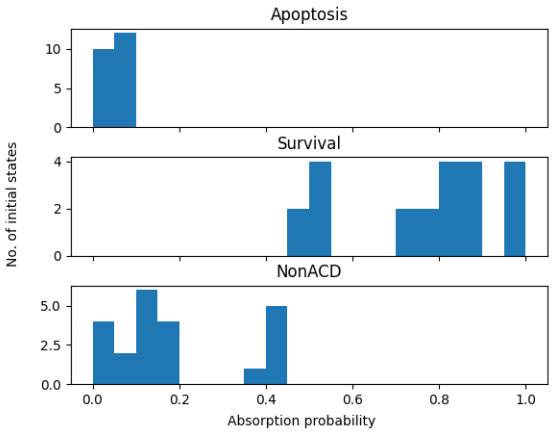

Figure 13: Distribution of absorption probabilities for 22 selected initial states of the network with $TNF \rightarrow C8$ edge tuned with $\theta = 0.8$. STG for the tuned network was generated as an average of 20 BM-ProSPR re-initializations.

5.6 Inferring roles of nodes in apoptotic response sensitivity among selected network states

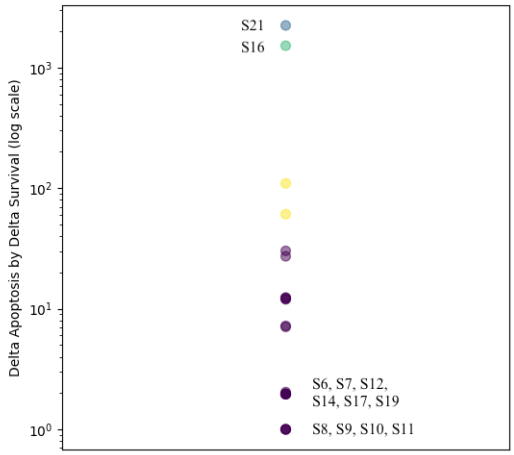

Figure 14: Clustering of the 22 states in Table 6 based on their ΔABP_{ratio} values for WT network vs. $RIP1 \rightarrow ROS$ tuned network with $\theta = 0.8$.

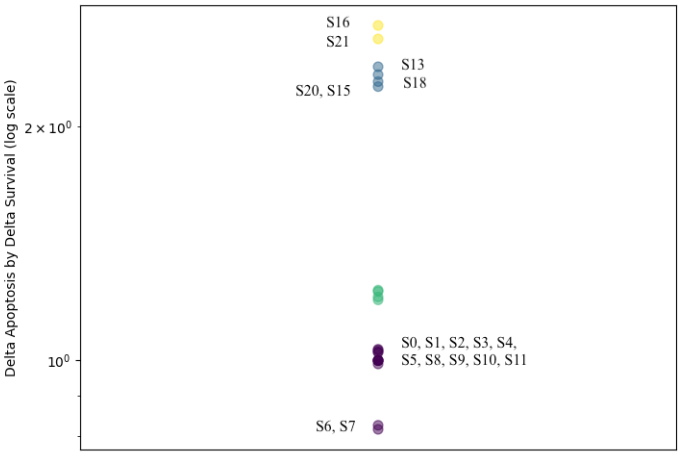

Figure 15: Clustering of the 22 states in Table 6 based on their ΔABP_{ratio} values for the WT network given in Figure 3 compared to the $TNF \rightarrow C8$ edge-tuned network with $\theta = 0.8$.

On closer observation of Table 3, one can make the following inferences with respect to these 22 selected initial states:

- All 22 states have the 6th node = 1 (i.e. cIAP is active)
- Primarily these states have the 4th node active (corresponding to NFkB/survival)
- Only 2 states have the 8th node active (corresponding to C3/apoptosis)

- Only 2 states have the 10th node active (corresponding to MOMP)

Taking both the single-edge perturbation cases considered previously, i.e. $RIP1 \rightarrow ROS$ with $\theta = 0.8$, and $TNF \rightarrow CASP8$ with $\theta = 0.8$, calculating ΔABP_{ratio} for these 22 states in each case, the resulting values are shown in a clustered form in Figures 14 and 15 respectively.

Upon clustering, S16 and S21 show maximum ΔABP_{ratio} in both cases. S16 (10111100110) and S21 (10111110110) are thus the most sensitive in their apoptotic response change, and S6, S7, S8, S9, S10, S11 are overall the least sensitive.

S	TNF	FAS	RIP1	NFkB	C8	cIAP	ATP	C3	ROS	MOMP	MPT
S16	1	0	1	1	1	1	0	0	1	1	0
S14	1	0	1	1	1	1	0	0	1	0	0
S21	1	0	1	1	1	1	1	0	1	1	0
S19	1	0	1	1	1	1	1	0	1	0	0

Table 4: Identifying nodes that make network states S16 and S21 highly sensitive to perturbation in their apoptosis vs. survival response.

S16 and S21 differ at a single node, ATP (i.e. they have a hamming distance $H = 1$). Hence ATP is not key in making both these states sensitive. Within the 22 initial states being considered, S14 also has a hamming distance $H = 1$ from S16, differing at the node MOMP. S19 has a hamming distance $H = 1$ from S21, also differing from S21 at the same node MOMP (see Table 4). Since S14 and S19 both show low ΔABP_{ratio} values, we can infer that MOMP being in an ON/active mode is critical to making the network state highly sensitive to perturbation.

States S6, S7, S8, S9, S10, S11 are least sensitive in both cases. Along with MOMP, all of these also have $C8 = 0$, whereas it is $C8 = 1$ in S16 and S21 (see Table 5). RIP1, clAP, CASP3 and MPT are the same regardless of the state's sensitivity level, possibly indicating that these nodes do not play a significant role in making a state sensitive to apoptotic response.

S	TNF	FAS	RIP1	NFkB	C8	cIAP	ATP	C3	ROS	MOMP	MPT
S16	1	0	1	1	1	1	0	0	1	1	0
S21	1	0	1	1	1	1	1	0	1	1	0
S6	1	0	1	0	0	1	0	0	0	0	0
S7	1	0	1	0	0	1	1	0	0	0	0
S8	1	0	1	1	0	1	0	0	0	0	0
S9	1	0	1	1	0	1	0	0	1	0	0
S10	1	0	1	1	0	1	1	0	1	0	0

Table 5: Identifying nodes that make network states S6, S7, S8, S9, S10, S11 minimally sensitive to perturbation in their apoptosis vs. survival response compared to S16 and S21.

5.7 Inferring roles of nodes in apoptotic response sensitivity among all network states

To get a more complete understanding of which nodes are key in making a state more sensitive to network perturbation, all those initial states among the total 512 of the network with $H = 1$ from each of S16 and S21 are also checked for their ABP_{ratio} values.

First considering S16, there are 9 initial states at $H = 1$ from this state (since cases where $TNF = 0$ or $FAS = 1$ are not considered). These states are denoted as $S'0, S'1, S'2, \ldots, S'8$ in the following analysis. The clustering of ΔABP_{ratio} values for these 9 states under each of a $RIP1 \rightarrow ROS$ tuned network with $\theta = 0.8$ and a $TNF \rightarrow C8$ tuned network with $\theta = 0.8$ are shown in Figures 16 and 17 respectively.

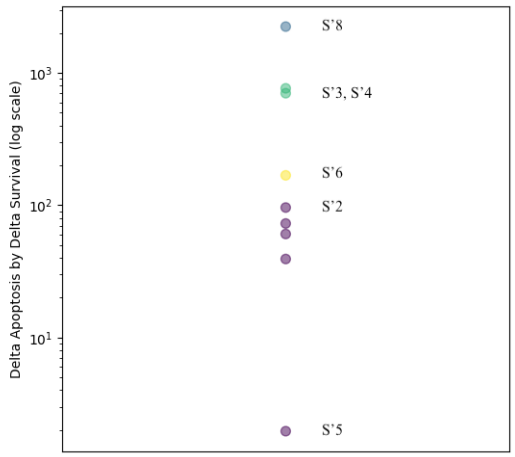

Figure 16: Clustering of all states with $H = 1$ from S16 (except those where $TNF = 0$ or $FAS = 1$) based on their ΔABP_{ratio} values for WT network vs. $RIP1 \rightarrow ROS$ tuned network with $\theta = 0.8$.

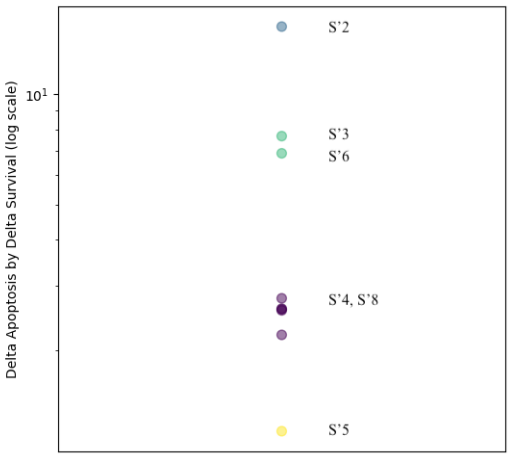

Figure 17: Clustering of all states with $H = 1$ from S16 (except those where $TNF = 0$ or $FAS = 1$) based on their ΔABP_{ratio} values for WT network vs. $TNF \rightarrow CASP8$ edge-tuned network with $\theta = 0.8$.

$S'2, S'3$ and $S'6$ show an overall high ΔABP_{ratio} in both edge-tuning cases, and $S'5$ shows the lowest value in both cases. A comparison of the values of all 11 nodes in these states with S16 is provided in Table 6.

S	TNF	FAS	RIP1	NFkB	C8	cIAP	ATP	C3	ROS	MOMP	MPT
S16	1	0	1	1	1	1	0	0	1	1	0
S′2	1	0	1	1	0	1	0	0	1	1	0
S′3	1	0	1	1	1	0	0	0	1	1	0
S′6	1	0	1	1	1	1	0	0	1	1	1
S′5	1	0	1	1	1	1	0	0	1	0	0

Table 6: Identifying nodes that make network states S′2, S′3, S′6 more sensitive (similar to S16) and S′5 minimally sensitive to perturbation in their apoptosis vs. survival response.

$S'5$ having $MOMP = 0$, whereas the remaining states have $MOMP = 1$, provides further evidence for MOMP playing a role in increasing sensitivity. On the other hand, C8, clAP and MPT do not appear to have a significant role in increasing sensitivity.

Next considering S21, there are again 9 initial states at $H = 1$ from this state (since cases where $TNF = 0$ or $FAS = 1$ are not considered). These states are now denoted as $S'0, S'1, S'2, \ldots, S'8$ in the following analysis. The clustering of ΔABP_{ratio} values for these 9 states under each of a

$RIP1 \to ROS$ tuned network with $\theta = 0.8$ and a $TNF \to C8$ tuned network with $\theta = 0.8$ are shown in Figures 18 and 19 respectively.

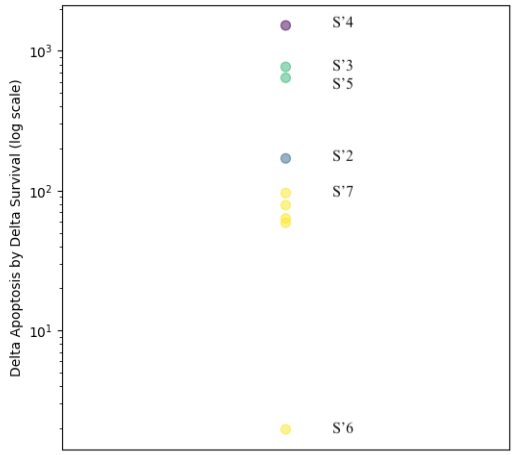

Figure 18: Clustering of all states with $H = 1$ from S21 (except those where $TNF = 0$ or $FAS = 1$) based on their ΔABP_{ratio} values for WT network vs. $RIP1 \to ROS$ tuned network with $\theta = 0.8$.

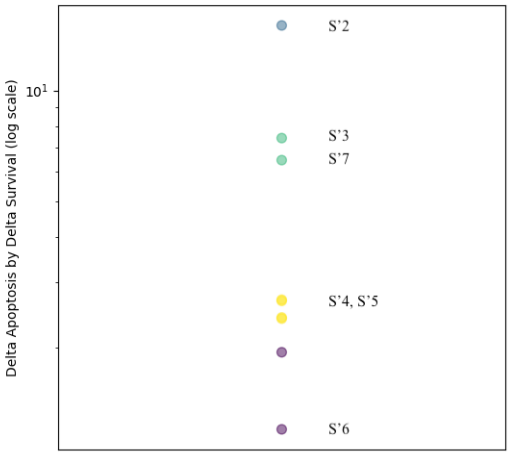

Figure 19: Clustering of all states with $H = 1$ from S21 (except those where $TNF = 0$ or $FAS = 1$) based on their ΔABP_{ratio} values for WT network vs. $TNF \to CASP8$ edge-tuned network with $\theta = 0.8$.

$S'2, S'3$ and $S'7$ show an overall high ΔABP_{ratio} in both edge-tuning cases, and $S'6$ shows the lowest value in both cases. A comparison of the values of all 11 nodes in these states with S21 is provided in Table 7.

S	TNF	FAS	RIP1	NFkB	C8	cIAP	ATP	C3	ROS	MOMP	MPT
S21	1	0	1	1	1	1	1	0	1	1	0
S′2	1	0	1	1	0	1	1	0	1	1	0
S′3	1	0	1	1	1	0	1	0	1	1	0
S′7	1	0	1	1	1	1	1	0	1	1	1
S′6	1	0	1	1	1	1	1	0	1	0	0

Table 7: Identifying nodes that make network states S′2, S′3, S′7 more sensitive (similar to S21) and S′6 minimally sensitive to perturbation in their apoptosis vs. survival response.

$S'6$ having $MOMP = 0$, whereas the remaining states have $MOMP = 1$, again confirms the role of MOMP in increasing sensitivity. Similar to the results from the previous analysis, C8, clAP and MPT do not appear to have a significant role in increasing sensitivity.

6 Fifteen-node network

6.1 Network definition

Taking into consideration more detailed literature, a 15-node network whose boolean rules are described in Table 8 is analyzed next. To get this network from the previous 11-node network,

the nodes FAS and cIAP present in the 11-node network are removed, and six new nodes are added (XIAP, JNK, AKT, Ceramide, PI3K, and Bax). TNF remains as the sole input node, with its value always set to 1.

Node	Boolean rule
TNF	Input node (always set to ON)
$RIP1$	$\neg C8 \wedge TNF$
$NFkB$	$RIP1 \wedge \neg C3$
$C8$	$(TNF \wedge \neg NFkB) \vee C3$
ATP	$\neg MPT$
$C3$	$(ATP \wedge MOMP) \wedge \neg(XIAP \vee AKT)$
ROS	$(RIP1 \vee MPT) \wedge \neg NFkB$
$MOMP$	$MPT \vee (C8 \wedge \neg NFkB$
MPT	$ROS \wedge \neg NFkB$
$XIAP$	$NFkB \wedge \neg Bax$
JNK	$Ceramimde \wedge \neg(AKT \vee XIAP)$
AKT	$PI3K \wedge \neg Ceramide$
$Ceramide$	$\neg PI3K \wedge TNF$
$PI3K$	$NFkB$
Bax	$\neg AKT$

Table 8: Boolean rules of the 15-node network. TNF is an input node always set to 1 here.

6.2 RIP1 → ROS edge tuning

Considering this 15-node WT network, BM-ProSPR is run with $TNF = 1$ to generate the STG and thus calculate the absorption probability to the three steady states Survival (S), NonACD (N), and Apoptosis (A) for each of the 2^{14} initial network states. The obtained distribution of absorption probabilities is shown in Figure 20.

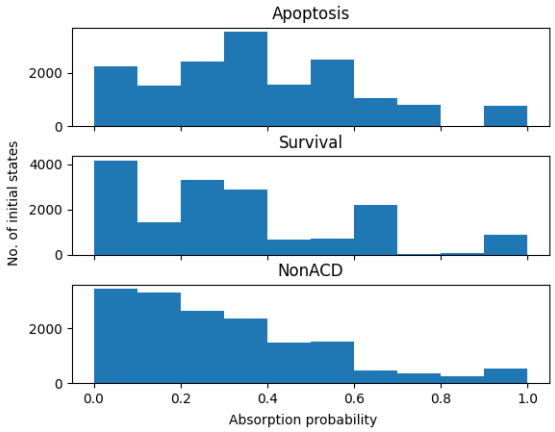

Figure 20: Distribution of absorption probabilities for all 2^{14} initial states of the wild-type network described in Table 8 with $TNF = 1$. STG for the network was generated from 1 run of BM-ProSPR.

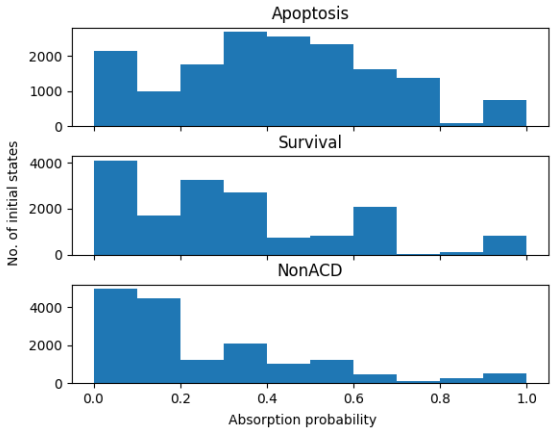

Figure 21: Distribution of absorption probabilities for 2^{14} initial states of the network with $RIP1 \rightarrow ROS$ edge tuned with $\theta = 0.6$. STG for the tuned network was generated from 1 run of BM-ProSPR.

Working with the assumption that edge inhibition cannot be complete, the $RIP1 \rightarrow ROS$

edge is tuned with $\theta = 0.6$. The resulting distribution of absorption probabilities after running BM-ProSPR on this network is shown in Figure 21.

Comparing the two figures, an overall increase in $ABP_{Apoptosis}$ can be seen. This is compensated by a decrease in ABP_{NonACD}, since there is no significant change in $ABP_{Survival}$.

This is repeated for all values of $\theta \in \{0.0, 0.1, 0.2, 0.3, \ldots, 0.9, 1.0\}$. As θ increases, a monotonic right-ward shift of the $ABP_{Apoptosis}$ distribution is seen, along with a monotonic left-ward shift of the ABP_{NonACD} distribution. This increase of apoptosis probability with respect to survival probability on inhibition of the direct $RIP1 \rightarrow ROS$ interaction is consistent with the results obtained from the 11-node network, and results seen in existing literature.

6.3 TNF → C8 edge tuning

The same process is carried out with a perturbed network where the tuned edge is $TNF \rightarrow CASP8$ with $\theta = 0.6$ again. The absorption probability distributions for all 2^{14} states in the WT and perturbed network can be seen in Figures 22 and 23 respectively.

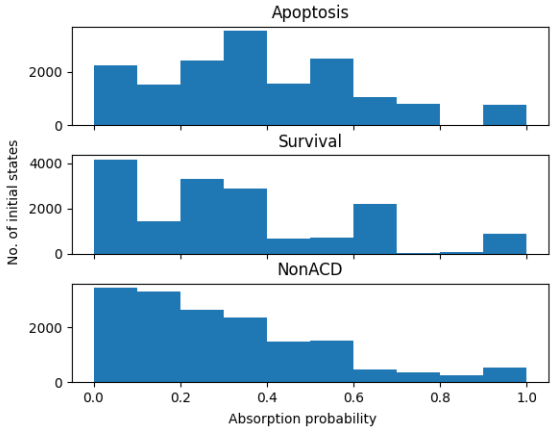

Figure 22: Distribution of absorption probabilities for all 2^{14} initial states of the wild-type 15-node network with $TNF = 1$. STG for the network was generated from 1 run of BM-ProSPR.

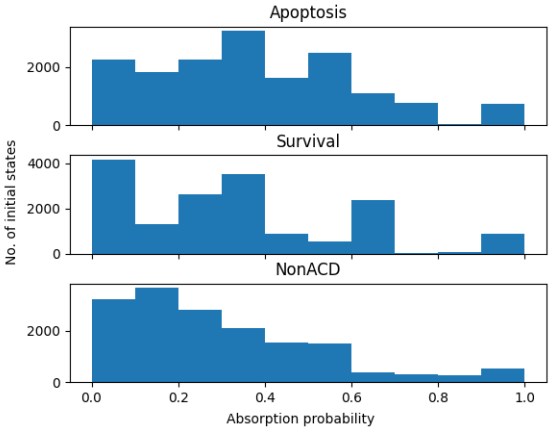

Figure 23: Distribution of absorption probabilities for 2^{14} initial states of the network with $TNF \rightarrow C8$ edge tuned with $\theta = 0.6$. STG for the tuned network was generated from 1 run of BM-ProSPR.

Here, there is a moderate decrease of $ABP_{Apoptosis}$ compensated by an increase in ABP_{NonACD}, with negligible change in the distribution of $ABP_{Survival}$ once again.

This is repeated for all values of $\theta \in \{0.0, 0.1, 0.2, 0.3, \ldots, 0.9, 1.0\}$. As θ increases, a monotonic left-ward shift of the $ABP_{Apoptosis}$ distribution is seen, along with a monotonic right-ward shift of the ABP_{NonACD} distribution. These results are also consistent with those obtained from the 11-node network, and those seen in existing literature.

6.4 Selecting initial network states for analysis of shift in cell fate

To further analyze those initial states in particular that are biologically relevant, i.e. their absorption probabilities reflect those seen in experiments, we once again select those states s in the WT network that fulfill Equation 6.

This condition is fulfilled by 4082 out of the 2^{14} initial network states. These states are denoted as $S_0, S_1, S_2, \ldots, S_{4080}, S_{4081}$ in the following analysis.

The shift in the distribution of absorption probabilities for only these 4082 states on carrying out edge tuning of $RIP1 \rightarrow ROS$ with $\theta = 0.6$ is checked. Relative to the WT network (Figure 24), we again see an overall increase in $ABP_{Apoptosis}$ compensated by a decrease in ABP_{NonACD} in the edge-tuned network (Figure 25), with less significant changes in $ABP_{Survival}$.

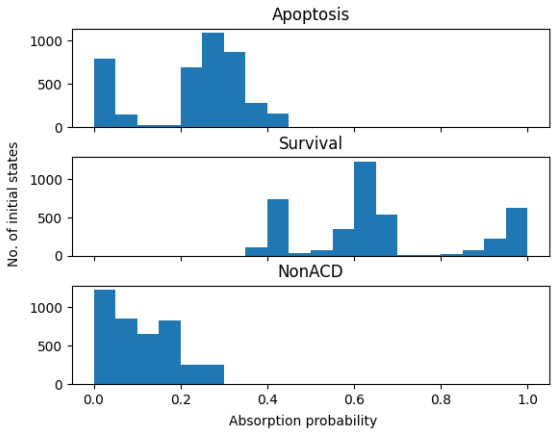

Figure 24: Distribution of absorption probabilities for 4082 selected initial states of the wild-type network with $TNF = 1$. STG for the network was generated from a single run of BM-ProSPR.

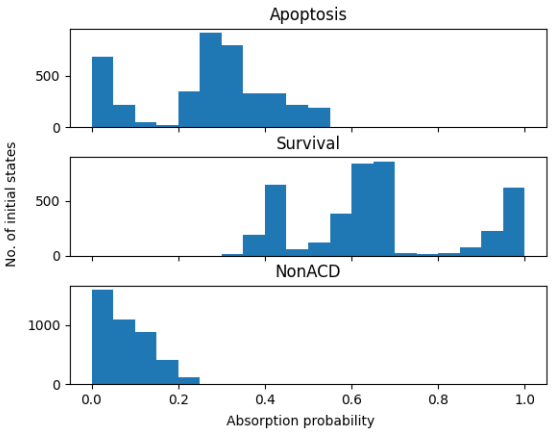

Figure 25: Distribution of absorption probabilities for 4082 selected initial states of the network with $RIP1 \rightarrow ROS$ edge tuned with $\theta = 0.6$. STG was generated from a single run of BM-ProSPR.

Repeating the same for the case with edge tuning of $TNF \rightarrow C8$ with $\theta = 0.6$, a similar shift to that observed when all 2^{14} initial states were considered is seen. This can be seen on comparing Figure 27 with Figure 26.

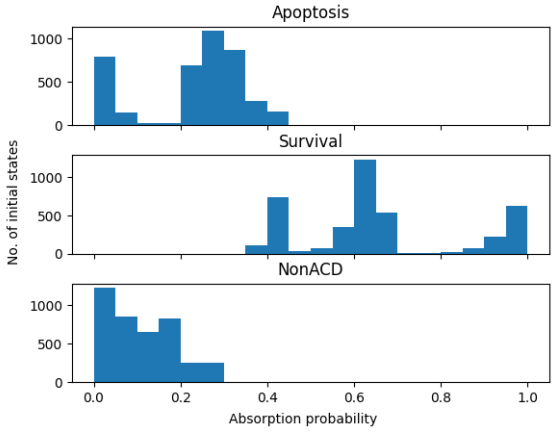

Figure 26: Distribution of absorption probabilities for 4082 selected initial states of the wild-type network with $TNF = 1$. STG for the network was generated from a single run of BM-ProSPR.

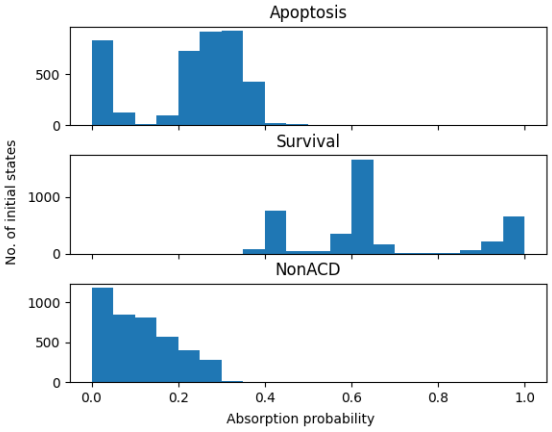

Figure 27: Distribution of absorption probabilities for 4082 selected initial states of the network with $TNF \rightarrow C8$ edge tuned with $\theta = 0.6$. STG was generated from one run of BM-ProSPR.

6.5 Inferring roles of nodes in apoptotic response sensitivity among selected network states

Taking both the single-edge perturbation cases considered previously, i.e. $RIP1 \rightarrow ROS$ with $\theta = 0.6$, and $TNF \rightarrow C8$ with $\theta = 0.6$, calculating ΔABP_{ratio} for the 4082 selected states in each case, the resulting values are shown in a clustered form in Figures 28 and 29 respectively.

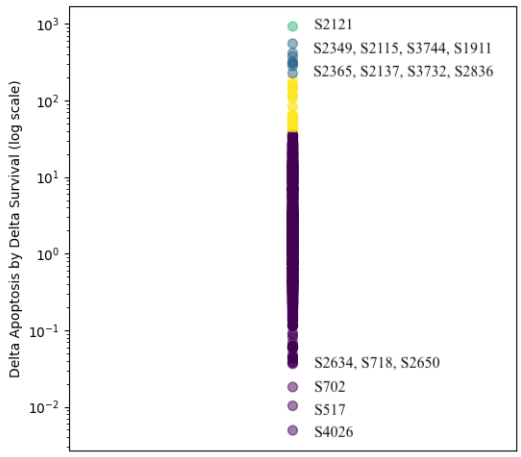

Figure 28: Clustering of the 4082 states based on their ΔABP_{ratio} values for the WT network compared to the $RIP1 \rightarrow ROS$ edge-tuned network with $\theta = 0.6$.

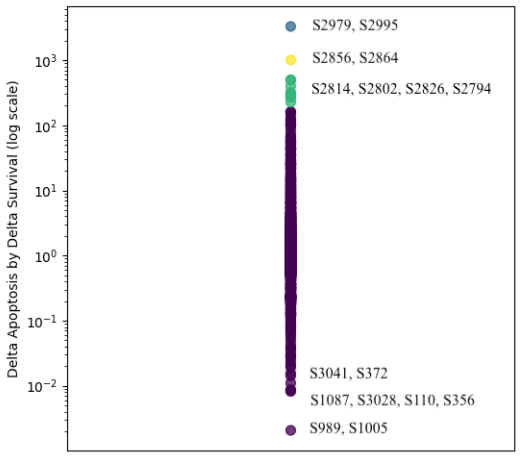

Figure 29: Clustering of the 4082 states based on their ΔABP_{ratio} values for the WT network compared to the $TNF \rightarrow C8$ edge-tuned network with $\theta = 0.6$.

Upon clustering, S2121, S2349 show the maximum and S4026, S517 show the minimum ΔABP_{ratio} for the $RIP1 \rightarrow ROS$ edge-tuned network. For the $TNF \rightarrow C8$ edge-tuned network, S2979, 2995 show the maximum ΔABP_{ratio}, and S989, S1005 show the minimum. A comparison of the node values for all these states is shown in Table 9.

There is not yet a clear conclusion on the roles of the nodes in sensitivity to perturbation by $RIP1 \rightarrow ROS$ tuning from states S2121, S2349, S4026, S517. However, on perturbation by $TNF \rightarrow C8$ tuning, there is a clear division between the highly and minimally sensitive states with respect to their values of NFkB, ATP, C3, ROS, MOMP, AKT and Ceramide.

6.6 Inferring roles of nodes in apoptotic response sensitivity among all network states

To get a more complete understanding of which nodes are key in making a state more sensitive to network perturbation, all those initial states among the total 2^{14} of the network with $H = 1$ from each of S2121, S2349 (in the case of $RIP1 \rightarrow ROS$ tuning) and S2979, S2995 (in the case of $TNF \rightarrow C8$ tuning) are also checked for their ABP_{ratio} values.

First considering S2121 and S2349, there are 14 initial states at $H = 1$ from each of these states (since the case where $TNF = 0$ is not considered). These two sets of 14 states are respectively denoted as $S'0, S'1, S'2, \ldots, S'13$ and $T'0, T'1, T'2, \ldots, T'13$ in the following analysis. The clusterings of ΔABP_{ratio} values for these two sets of 14 states under a $RIP1 \rightarrow ROS$ tuned network with $\theta = 0.6$ are shown in Figures 30 and 31 respectively.

Node	RIP1 → ROS tuning				TNF → C8 tuning			
	S2121	**S2349**	**S4026**	**S517**	**S2979**	**S2995**	**S989**	**S1005**
TNF	1	1	1	1	1	1	1	1
RIP1	1	1	1	0	1	1	1	1
NFkB	1	1	1	1	1	1	0	0
C8	0	0	1	0	0	0	0	0
ATP	0	1	1	1	1	1	0	0
C3	1	0	0	0	1	1	0	0
ROS	1	0	1	0	1	1	0	0
MOMP	1	1	1	1	0	0	1	1
MPT	0	0	1	0	1	1	1	1
XIAP	1	0	0	0	1	1	1	1
JNK	0	0	0	0	0	1	0	1
AKT	0	0	0	1	1	1	0	0
Ceramide	0	1	0	0	0	0	1	1
PI3K	1	1	1	0	1	1	1	1
Bax	1	1	1	0	1	1	1	1

Table 9: Identifying nodes that make particular network states among the 4082 highly or minimally sensitive to perturbation in their apoptosis vs. survival response.

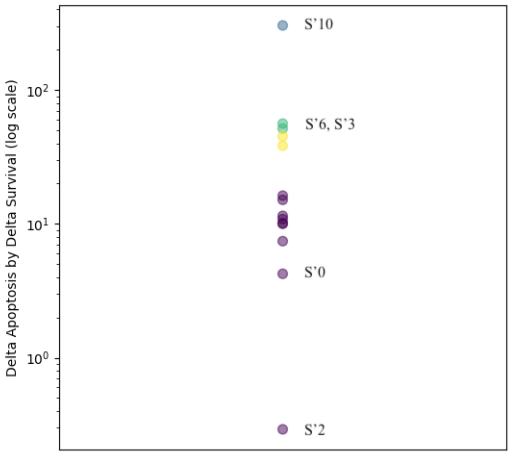

Figure 30: Clustering of all states with $H = 1$ from S2121 (except the one where $TNF = 0$) based on their ΔABP_{ratio} values for WT network vs. $RIP1 \rightarrow ROS$ tuned network with $\theta = 0.6$.

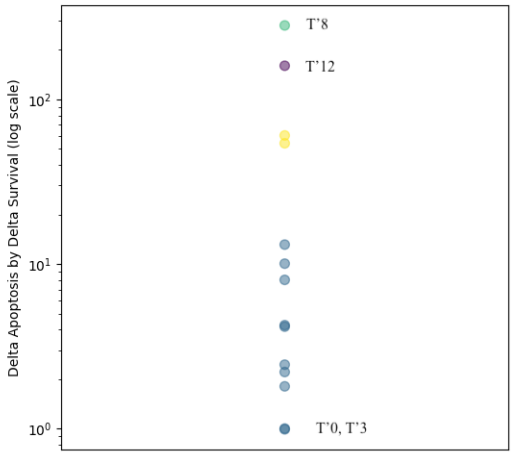

Figure 31: Clustering of all states with $H = 1$ from S2349 (except the one where $TNF = 0$) based on their ΔABP_{ratio} values for WT network vs. $RIP1 \rightarrow ROS$ edge-tuned network with $\theta = 0.6$.

$S'10, S'6, T'8, T'12$ show relatively high ΔABP_{ratio} values, and $S'0, S'2, T'0, T'3$ the lowest values. A comparison of the values of all 15 nodes in these states with those in S2121 and S2349 is provided in Table 10.

Node	S2121	H = 1 from S2121				S2349	H = 1 from S2349			
		S′10	S′6	S′0	S′2		T′8	T′12	T′0	T′3
TNF	1	1	1	1	1	1	1	1	1	1
RIP1	1	1	1	0	1	1	1	1	0	1
NFkB	1	1	1	1	1	1	1	1	1	1
C8	0	0	0	0	0	0	0	0	0	0
ATP	0	0	0	0	0	1	1	1	1	1
C3	1	1	1	1	0	0	0	1	0	0
ROS	1	1	1	1	1	0	0	0	0	0
MOMP	1	1	1	1	1	1	1	1	1	0
MPT	0	0	0	0	0	0	0	0	0	0
XIAP	1	1	1	1	1	0	0	0	0	0
JNK	0	1	0	0	0	0	1	0	0	0
AKT	0	0	0	0	0	0	0	0	0	0
Ceramide	0	0	0	0	0	1	1	1	1	1
PI3K	1	1	0	1	1	1	1	1	1	1
Bax	1	1	1	1	1	1	1	1	1	1

Table 10: Identifying nodes that make S2121 and S2349 highly sensitive to perturbation via $RIP1 \rightarrow ROS$ tuning with $\theta = 0.6$ in their apoptosis vs. survival response, compared to other states at $H = 1$ from them.

$NFkB$ does not appear to affect sensitivity, since it is $= 1$ for all states. Similarly, $C8, Bax$, MPT and AKT also have the same value throughout. $RIP1$ appears to have some role in increasing sensitivity, as the states with the respective lowest ΔABP_{ratio} values in both cases ($S'0$ and $T'0$) are the only ones with $RIP1 = 0$.

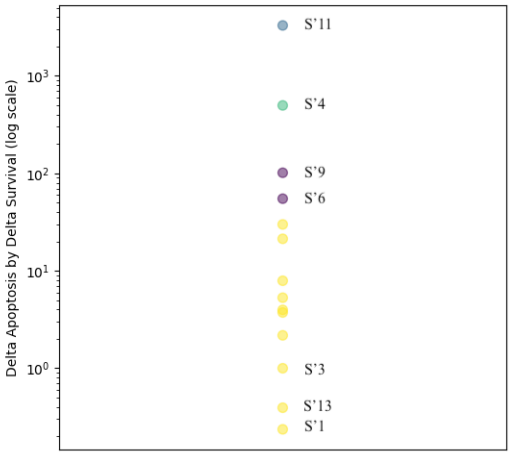

Figure 32: Clustering of all states with $H = 1$ from S2979 (except the one where $TNF = 0$) based on their ΔABP_{ratio} values for WT network vs. $TNF \rightarrow C8$ edge-tuned network with $\theta = 0.6$.

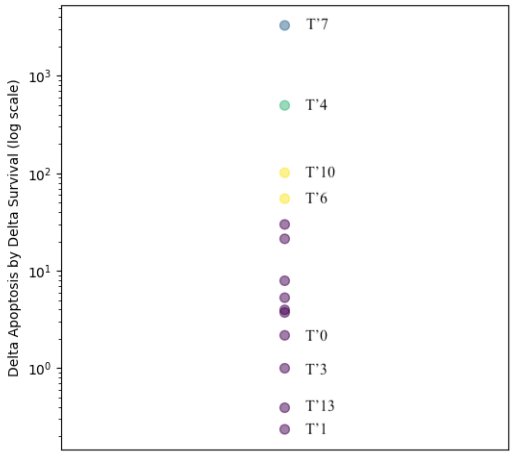

Figure 33: Clustering of all states with $H = 1$ from S2995 (except the one where $TNF = 0$) based on their ΔABP_{ratio} values for WT network vs. $TNF \rightarrow C8$ edge-tuned network with $\theta = 0.6$.

Next considering S2979 and S2995, there are again 14 initial states at $H = 1$ from each of

these states (since the case where $TNF = 0$ is not considered). These two sets of 14 states are now respectively denoted as $S'0, S'1, S'2, \ldots, S'13$ and $T'0, T'1, T'2, \ldots, T'13$ in the following analysis. The clusterings of ΔABP_{ratio} values for these two sets of 14 states under a $TNF \rightarrow C8$ tuned network with $\theta = 0.6$ are shown in Figures 32 and 33 respectively.

$S'11, S'4, T'7, T'4$ show relatievly high ΔABP_{ratio} values, and $S'1, S'13, T'1, T'13$ the lowest values. A comparison of the values of all 15 nodes in these states with those in S2979 and S2995 is provided in Table 11.

ROS and JNK do not appear to affect sensitivity. Here, $NFkB$ appears to have some role in increasing sensitivity, as the states with the respective lowest ΔABP_{ratio} values in both cases ($S'1$ and $T'1$) are the only ones with $NFkB = 0$.

Node	**S2979**	**H = 1 from S2979**				**S2995**	**H = 1 from S995**			
		S′11	**S′4**	**S′1**	**S′13**		**T′7**	**T′4**	**T′1**	**T′13**
TNF	1	1	1	1	1	1	1	1	1	1
RIP1	1	1	1	1	1	1	1	1	1	1
NFkB	1	1	1	0	1	1	1	1	0	1
C8	0	0	0	0	1	0	0	0	0	1
ATP	1	1	1	1	1	1	1	1	1	1
C3	1	1	1	1	1	1	1	1	1	1
ROS	1	1	0	1	1	1	1	0	1	1
MOMP	0	0	0	0	0	0	0	0	0	0
MPT	1	1	1	1	1	1	1	1	1	1
XIAP	1	1	1	1	1	1	1	1	1	1
JNK	0	1	0	0	0	1	0	1	1	1
AKT	1	1	1	1	1	1	1	1	1	1
Ceramide	0	0	0	0	0	0	0	0	0	0
PI3K	1	1	1	1	1	1	1	1	1	1
Bax	1	1	1	1	1	1	1	1	1	1

Table 11: Identifying nodes that make S2979 and S2995 highly sensitive to perturbation via $TNF \rightarrow C8$ tuning with $\theta = 0.6$ in their apoptosis vs. survival response, compared to other states at $H = 1$ from them.

7 Conclusions and future work

Perturbing the $RIP1 \rightarrow ROS$ and $TNF \rightarrow C8$ edges reproduces experimentally observed shifts in cell fate distribution (qualitatively), in both the 11-node network and the 15-node network. By identifying network states that, on performing these edge perturbations, show a large change in $ABP_{Apoptosis}$ compared to $ABP_{Survival}$, we can infer that MOMP being ON is critical to making these states sensitive in the 11-node network.

While some patterns have been observed for the 15-node network as well, identifying which nodes most strongly influence ABP_{ratio} values here, as well as the roles of other nodes in the 11-node network, requires a greater depth of analysis.

References

[1] Deritei D, Kunšič N, and Csermely P. Probabilistic edge weights fine-tune boolean network dynamics. *PLoS Comput Biol*, 18(10):e1010536, 2022.

[2] Shubhank Sherekar and Ganesh A. Viswanathan. Boolean dynamic modeling of cancer signaling networks: Prognosis, progression, and therapeutics. *Computational and Systems Oncology*, 1(2), 2021.

[3] Assieh Saadatpour and Réka Albert. Boolean modeling of biological regulatory networks: A methodology tutorial. *Methods*, 62(1):3–12, 2013. Modeling Gene Expression.

[4] Shubhank Sherekar and Ganesh Viswanathan. Boolean dynamic modeling of tnfr1 signaling predicts a nested feedback loop regulating the apoptotic response at single-cell level. *bioRxiv*, 2022.

[5] Calzone L, Tournier L, Fourquet S, Thieffry D, Zhivotovsky B, and et al Barillot E. Mathematical modelling of cell-fate decision in response to death receptor engagement. *PLoS Comput Biol*, 6(3):e1000702, 2010.